Panel method predictions of added mass for flexible airship

M. Zhang
wangxiaoliang@sjtu.edu.cn
X. Wang and D. Duan
School of Aeronautics and Astronautics
Shanghai Jiao Tong University
Shanghai, China

ABSTRACT

Because of the huge volume and inflated membrane structure of stratosphere airship, the deformation of stratosphere airship is very sensitive to the change of environment conditions such as wind, temperature and so on. The influence of deformation on manipulation and control is very remarkable. So, during the course of building flight dynamic model of the flexible airship, the added-mass matrix of deformation is very important part in the state equations of dynamic models. For obtaining the accurate added-mass matrix of different flexible airship, we proposed an approach that can calculate the added-mass matrix of a flexible airship with arbitrary geometry shape by the panel method. Through the comparison of results of computation and theory for ellipsoid of revolution and the flexible Skyship-500 airship, the proposed method can calculate the added-mass matrix for arbitrary geometric shape very accurately.

1.0 INTRODUCTION

With the development of correlative technology, there are some interests in an airship. Particularly, stratosphere airships can be used in some fields and were studied in the world nowadays. These class vehicles use the buoyancy as the lift, so they can flight with very slow velocity and keep station in the sky.

Because of the very small density of air in the stratosphere (0·0889 kg/m^3 at 20km), the volume of stratosphere airships is very huge. The main structure is inflated membrane and relatively small pressure difference is used thinking of the material characteristics and helium leakage. So, the deformation of stratosphere airship is very sensitive to the change of environment conditions such as wind, temperature and so on.

Paper No. 3833. Manuscript received 22 March 2012, revised version received 28 July 2012, accepted 9 August 2012.

https://doi.org/10.1017/S0001924000008162 Published online by Cambridge University Press

The deformation of stratosphere airship has influence on the structural stability and load distribution. Moreover, the deformation will change the capability of manipulation and control. The airship can not be controlled under the conditions of disabled rudder or elevator because of the large deformation of the airship. For the purpose of obtaining precision control, the building of a flight dynamic model of flexible stratosphere airship is very important. The deformation factor of this class of vehicle should be thought during the course of building the dynamic model.

Many researchers[1-7] built the dynamic model of airship under the hypothesis of rigid body condition. Yuwen Li[8] built the dynamic model of flexible airship, the structural deformations are calculated through the mode superposition method.

Building dynamic model of the flexible airship, the added-mass matrix of deformations is a very important part in the state equations. Yuwen Li[9] obtained the equations of element of added-mass matrix through the derivation and the analytical solution of an ellipsoid of revolution is applied to obtain the approximate results of a flexible airship with same fineness.

For obtaining the accurate added-mass matrix of different airship shape, we proposed an approach that can calculate the added-mass matrix of a flexible airship with arbitrary geometry shape through the panel method. This method can be used to solve the Laplace equation with different boundary conditions. Through the comparison of results of computation and theory for ellipsoid of revolution and the flexible Skyship-500 airship, the proposed method was verified. This method can calculate the added-mass matrix accurately for arbitrary geometric shape.

This paper is organized as follows: The equations and the calculate method of elements of an added mass matrix of flexible body was described in Section 2. The capability of the proposed method to calculate the added masses was validated in Section 3. The added-mass matrixes of airships with different geometric shapes were analysed in Section 4. In the final section, we draw some conclusions about computational method and added mass characteristics of flexible airships.

2.0 THE EQUATIONS AND CALCULATION METHOD OF ADDED MASS OF FLEXIBLE BODY

2.1 The added-mass matrix of the flexible body[9]

For obtaining the added-mass matrix of the flexible body, we can derive from the kinetic energy of the fluid T_f. The kinetic energy of the fluid is written as

$$T_f = \frac{1}{2}\rho_f \iiint_{Vol_f} (\mathbf{v}_f)^T (\mathbf{v}_f) \mathrm{d}Vol \qquad \ldots (1)$$

Where, ρ_f is the density of fluid, $\mathbf{v_f} = [u_f, v_f, w_f]^T$ is the velocity vector of fluid, Vol_f is the volume of fluid.

For a potential fluid, the velocity vector of the fluid $\mathbf{v_f}$ can be represented by the gradient of a scalar potential function Ψ, Using Green's theorem, the kinetic energy of the fluid can be expressed as,

$$T_f = \frac{1}{2}\rho_f \iiint_{Vol_f} (\mathbf{v}_f)^T (\mathbf{v}_f) \mathrm{d}Vol = \frac{1}{2}\rho_f \iiint_{Vol_f} (\nabla\psi)^T (\nabla\psi) \mathrm{d}Vol = -\frac{1}{2}\rho_f \iint_{S_B} \psi \frac{\partial\psi}{\partial n} \mathrm{d}S \qquad \ldots (2)$$

Where, S_B is the surface of the flexible body.

Based on the continuity equation for the fluid, the potential function can be written as the Laplace Equation [10].

https://doi.org/10.1017/S0001924000008162 Published online by Cambridge University Press

$$\nabla^2\psi = 0 \quad \ldots (3)$$

The boundary condition of Equation (4) is the normal component of the fluid velocity must be equal to the normal velocity of the body on every location of the body surface.

$$\mathbf{v}_f{}^T\mathbf{n} = \mathbf{v}_d{}^T\mathbf{n} \quad \ldots (4)$$

Where, $\mathbf{v_d}$ is the surface velocity of the flexible body. $\mathbf{n} = [n_1, n_2, n_1]^T$ is the unit normal vector of the boundary surface, with its positive direction defined outside the body .

The velocity distribution along the flexible body[9] is,

$$\mathbf{v}_d \approx \mathbf{v}_0 + \omega^{\times}\mathbf{r} + \sum_{i=1}^{N}\dot{q}_i\Phi_i - u_0\sum_{i=1}^{N}q_i\Phi_i' \quad \ldots (5)$$

Where, $\mathbf{v_0} = [u_0, v_0, w_0]^T$ is the linear velocity vector, $\boldsymbol{\omega} = [p, q, r]^T$ is the angular velocity vector, $\boldsymbol{\omega}^{\mathrm{x}}$ is the antisymmetric cross-product matrix

$$\omega^{\times} = \begin{bmatrix} 0 & -r & q \\ r & 0 & -p \\ -q & p & 0 \end{bmatrix},$$

$\mathbf{r} = [x, y, z]^T$ is position vector of a body surface point from the body-frame origin on the undeformed body, q_i is the generalised co-ordinate, Φ_i is the ith mode shape function, $\Phi'_i = \mathrm{d}\Phi/\mathrm{d}x$,$N$, is the number of mode shape functions describing the deformation.

Substituting $\mathbf{v_d}$ from Equation (5) into Equation (4), we have

$$\begin{aligned}\mathbf{v}_f{}^T\mathbf{n} &= (\mathbf{v}_0 + \omega^{\times}\mathbf{r} + \sum_{i=1}^{N}\dot{q}_i\Phi_i - u_0\sum_{i=1}^{N}q_i\Phi_i')^T\mathbf{n} \\ &= \mathbf{v}_0{}^T\mathbf{n} + \omega^T(\mathbf{r}^{\times}\mathbf{n}) + \sum_{i=1}^{N}\dot{q}_i\Phi_i{}^T\mathbf{n} - u_0\sum_{i=1}^{N}q_i\Phi'^T\mathbf{n}\end{aligned} \quad \ldots (6)$$

Equation (6) represents the boundary conditions of the Laplace equation for a flexible body moving through an unbounded potential fluid.

Based on the superposition theory and the boundary condition Equation (6), the total velocity potential Ψ can be written as,

$$\psi = \mathbf{v}^T\psi_r + \dot{\mathbf{q}}^T\psi_q + u_0\mathbf{q}^T\psi_s \quad \ldots (7)$$

Where, $\boldsymbol{\psi}_\mathbf{r} = [\psi_{r1}, \psi_{r2}, \ldots, \psi_{r6}]^T$ is the velocity potentials associated with the rigid-body motion, $\boldsymbol{\psi}_\mathbf{q} = [\psi_{q1}, \psi_{q2}, \ldots, \psi_{q6}]^T$ is the potential components related to the mode shapes. $\boldsymbol{\psi}_\mathbf{s} = [\psi_{s1}, \psi_{s2}, \ldots, \psi_{s6}]^T$ is the potential components associated with the slopes of the mode shape functions.

With the velocity potential in Equation (7), the kinetic energy of the fluid is

$$\begin{aligned}T_f &= -\frac{1}{2}\rho\iint_{S_B}\psi\frac{\partial\psi}{\partial n}\mathrm{d}S \\ &= -\frac{1}{2}\rho\iint_{S_B}(\mathbf{v}^T\psi_r + \dot{\mathbf{q}}^T\psi_q + u_0\mathbf{q}^T\psi_s)\frac{\partial(\mathbf{v}^T\psi_r + \dot{\mathbf{q}}^T\psi_q + u_0\mathbf{q}^T\psi_s)}{\partial n}\mathrm{d}S\end{aligned}$$

https://doi.org/10.1017/S0001924000008162 Published online by Cambridge University Press

$$\begin{aligned}
&= \frac{1}{2}\mathbf{v}^T M_{rr}\mathbf{v} + \frac{1}{2}\mathbf{v}^T M_{rq}\dot{\mathbf{q}} + \frac{1}{2}\mathbf{v}^T M_{rs}(u_0\mathbf{q}) \\
&+ \frac{1}{2}\dot{\mathbf{q}}^T M_{qr}\mathbf{v} + \frac{1}{2}\dot{\mathbf{q}}^T M_{qq}\dot{\mathbf{q}} + \frac{1}{2}\dot{\mathbf{q}}^T M_{qs}(u_0\mathbf{q}) \\
&+ \frac{1}{2}u_0\mathbf{q}^T M_{sr}\mathbf{v} + \frac{1}{2}u_0\mathbf{q}^T M_{sq}\dot{\mathbf{q}} + \frac{1}{2}u_0\mathbf{q}^T M_{ss}(u_0\mathbf{q}) \\
&= \frac{1}{2}\left[\mathbf{v}^T, \dot{\mathbf{q}}^T\right] M_{AT}\left[\mathbf{v}^T, \dot{\mathbf{q}}^T\right]^T
\end{aligned} \quad \ldots (8)$$

Where, $\mathbf{M_{qr}} = \mathbf{M_{rq}}^{\mathbf{T}}$, $\mathbf{M_{sr}} = \mathbf{M_{rs}}^{\mathbf{T}}$, $\mathbf{M_{rr}}$, $\mathbf{M_{rq}}$, $\mathbf{M_{rs}}$, $\mathbf{M_{qr}}$, $\mathbf{M_{qq}}$, $\mathbf{M_{qs}}$, $\mathbf{M_{sr}}$, $\mathbf{M_{sq}}$, $\mathbf{M_{ss}}$ are the added-mass matrixes of the flexible body. The detail expression equations of these elements of added-mass matrixes are,

$$M_{rr,ij} = -\rho \iint_{S_B} \psi_{ri} \frac{\partial \psi_{rj}}{\partial n} \mathrm{d}S \quad \ldots (9)$$

$$M_{rq,ij} = -\rho \iint_{S_B} \psi_{ri} \frac{\partial \psi_{qj}}{\partial n} \mathrm{d}S \quad \ldots (10)$$

$$M_{qr,ij} = -\rho \iint_{S_B} \psi_{qi} \frac{\partial \psi_{rj}}{\partial n} \mathrm{d}S \quad \ldots (11)$$

$$M_{qq,ij} = -\rho \iint_{S_B} \psi_{qi} \frac{\partial \psi_{qj}}{\partial n} \mathrm{d}S \quad \ldots (12)$$

$$M_{rs,ij} = -\rho \iint_{S_B} \psi_{ri} \frac{\partial \psi_{sj}}{\partial n} \mathrm{d}S \quad \ldots (13)$$

$$M_{sr,ij} = -\rho \iint_{S_B} \psi_{si} \frac{\partial \psi_{rj}}{\partial n} \mathrm{d}S \quad \ldots (14)$$

$$M_{qs,ij} = -\rho \iint_{S_B} \psi_{qi} \frac{\partial \psi_{sj}}{\partial n} \mathrm{d}S \quad \ldots (15)$$

$$M_{sq,ij} = -\rho \iint_{S_B} \psi_{si} \frac{\partial \psi_{qj}}{\partial n} \mathrm{d}S \quad \ldots (16)$$

$$M_{ss,ij} = -\rho \iint_{S_B} \psi_{si} \frac{\partial \psi_{sj}}{\partial n} \mathrm{d}S \quad \ldots (17)$$

The total added-mass matrix $\mathbf{M_{AT}}$ can be divided into four parts,

$$M_{AT} = M_{A1} + M_{A2} + M_{A3} + M_{A4} \quad \ldots (18)$$

Where,

$$M_{A1} = \begin{bmatrix} M_{rr(6\times6)} & M_{rq(6\times N)} \\ M_{qr(N\times6)} & M_{qq(N\times N)} \end{bmatrix}_{(6+N)\times(6+N)} \qquad M_{A2} = \begin{bmatrix} (M_{rs}\mathbf{q})_{(6\times1)} & 0_{(6\times(N-1))} \\ (M_{qs}\mathbf{q})_{(N\times1)} & 0_{(N\times(N-1))} \end{bmatrix}_{(6+N)\times(6+N)}$$

$$M_{A3} = \begin{bmatrix} (\mathbf{q}^T M_{sr})_{(1\times6)} & (\mathbf{q}^T M_{sq})_{(1\times N)} \\ 0_{((5+N)\times6)} & 0_{((5+N)\times N)} \end{bmatrix}_{(6+N)\times(6+N)} \qquad M_{A3} = \begin{bmatrix} (\mathbf{q}^T M_{ss}\mathbf{q})_{(1\times1)} & 0_{(1\times(5+N))} \\ 0_{((5+N)\times1)} & 0_{((5+N)\times(5+N))} \end{bmatrix}_{(6+N)\times(6+N)}$$

https://doi.org/10.1017/S0001924000008162 Published online by Cambridge University Press

The potential-flow aerodynamic forces and moments of flexible body can be derived from the Lagrange's equation,

$$\frac{\mathrm{d}}{\mathrm{d}t}\frac{\partial T_f}{\partial \mathbf{v}_0}+\omega^{\times}\frac{\partial T_f}{\partial \mathbf{v}_0}=-\mathbf{F}_A \quad ...(19)$$

$$\frac{\mathrm{d}}{\mathrm{d}t}\frac{\partial T_f}{\partial \omega}+\mathbf{v}_0^{\times}\frac{\partial T_f}{\partial \mathbf{v}_0}+\omega^{\times}\frac{\partial T_f}{\partial \omega}=-\mathbf{M}_A \quad ...(20)$$

$$\frac{\mathrm{d}}{\mathrm{d}t}\frac{\partial T_f}{\partial \dot{\mathbf{q}}}-\frac{\partial T_f}{\partial \mathbf{q}}=-\mathbf{Q}_A \quad ...(21)$$

Where, $\mathbf{F_A}$, $\mathbf{M_A}$ and $\mathbf{Q_A}$ are the aerodynamic force, aerodynamic moments and generalised forces on the body from the potential fluid respectively. Through the derivation (9), the expression of $\mathbf{F_A}$, $\mathbf{M_A}$ and $\mathbf{Q_A}$ are

$$\begin{bmatrix}\mathbf{F}_A\\ \mathbf{M}_A\\ \mathbf{Q}_A\end{bmatrix}=-M_{AT}\cdot\begin{bmatrix}\dot{\mathbf{v}}_0\\ \dot{\omega}\\ \ddot{\mathbf{q}}\end{bmatrix}+\begin{bmatrix}\mathbf{F}_{A,non}(\mathbf{v}_0,\omega,\mathbf{q},\dot{\mathbf{q}})\\ \mathbf{M}_{A,non}(\mathbf{v}_0,\omega,\mathbf{q},\dot{\mathbf{q}})\\ \mathbf{Q}_{A,non}(\mathbf{v}_0,\omega,\mathbf{q},\dot{\mathbf{q}})\end{bmatrix} \quad ...(22)$$

Where, the first term is the linear part related to the linear acceleration, angular acceleration and the elastic generalised co-ordinate acceleration. While the second term is the nonlinear part related to the state variables and generalised co-ordinates. The detail expression equation of nonlinear part can be found in Ref. 9.

For a rigid-body completely submerged in an unbounded potential fluid, the added-masses $\mathbf{M_{AT}}$ can be reduced to a 6×6 matrix $\mathbf{M_{rr}}$. The element of 6×6 added-mass matrix of rigid-body can be obtained through solving the Laplace equation using the panel method. For a flexible-body with its deformation described by the superposition of N mode shape functions, the added-mass matrixes representing the fluid kinetic energy should be a (6+N)×(6+N) matrix. For the flexible-body, the element of added-mass matrix can be obtained using the same approach, but the boundary conditions of Laplace equation are different.

For obtaining the elements of added-mass matrixes $\mathbf{M_{rr}} = \mathbf{M_{rq}}$, $\mathbf{M_{rs}}$, $\mathbf{M_{qr}}$, $\mathbf{M_{qq}}$, $\mathbf{M_{qs}}$, $\mathbf{M_{sr}}$, $\mathbf{M_{sq}}$, $\mathbf{M_{ss}}$, we need to obtain the velocity potentials $\boldsymbol{\psi}_\mathbf{r}$, $\boldsymbol{\psi}_\mathbf{q}$ and $\boldsymbol{\psi}_\mathbf{s}$ firstly.

The velocity potentials associated with the rigid-body motion $\boldsymbol{\psi}_\mathbf{r}$ are functions of position only and satisfy the Laplace equation

$$\nabla^2\psi_{ri}=0 \quad ...(23)$$

The components related to translation and rotation satisfy the boundary conditions respectively,

$$\frac{\partial\psi_{r1}}{\partial n}=n_1;\quad \frac{\partial\psi_{r2}}{\partial n}=n_2\quad \frac{\partial\psi_{r3}}{\partial n}=n_3; \quad ...(24)$$

$$\frac{\partial\psi_{r4}}{\partial n}=-zn_2+yn_3\ ;\ \frac{\partial\psi_{r5}}{\partial n}=zn_1-xn_3;\ \frac{\partial\psi_{r6}}{\partial n}=-yn_1+xn_2\ ; \quad ...(25)$$

The potential components related to the mode shapes $\boldsymbol{\psi}_\mathbf{q}$ are independent of time and satisfies the Laplace equation with the corresponding boundary condition as,

https://doi.org/10.1017/S0001924000008162 Published online by Cambridge University Press

$$\nabla^2 \psi_{qi} = 0 \qquad \ldots (26)$$

$$\frac{\partial \psi_{qi}}{\partial n} = ¦_i^T \mathbf{n} = \left[\Phi_{xi}(x), \Phi_{yi}(x), \Phi_{zi}(x) \right] \begin{bmatrix} n_1 \\ n_2 \\ n_3 \end{bmatrix}$$
$$= \Phi_{xi}(x) \cdot n_1 + \Phi_{yi}(x) \cdot n_2 + \Phi_{zi}(x) \cdot n_3, i = 1, 2, \cdots, N \qquad \ldots (27)$$

$\boldsymbol{\psi}_{\mathbf{s}}$ represents the potential components associated with the slopes of the shape functions. $\boldsymbol{\psi}_{\mathbf{si}}$ is also independent of time and satisfies the Laplace equation with the corresponding boundary condition as,

$$\nabla^2 \psi_{si} = 0 \qquad \ldots (28)$$

$$\frac{\partial \psi_{si}}{\partial n} = -\Phi_i'^T \mathbf{n} = -\left[\Phi'_{xi}(x), \Phi'_{yi}(x), \Phi'_{zi}(x) \right] \begin{bmatrix} n_1 \\ n_2 \\ n_3 \end{bmatrix}$$
$$= -\left[\frac{\mathrm{d}\Phi_{xi}(x)}{\mathrm{d}x} \cdot n_1 + \frac{\mathrm{d}\Phi_{yi}(x)}{\mathrm{d}x} \cdot n_2 + \frac{\mathrm{d}\Phi_{zi}(x)}{\mathrm{d}x} \cdot n_3 \right], i = 1, 2, \cdots, N \qquad \ldots (29)$$

When the velocity potentials $\boldsymbol{\psi}_{\mathbf{r}}$, $\boldsymbol{\psi}_{\mathbf{q}}$ and $\boldsymbol{\psi}_{\mathbf{s}}$ were obtained, we can use the Equations (8-17) to get the added-mass matrixes $\mathbf{M}_{\mathbf{rr}}$, $\mathbf{M}_{\mathbf{rq}}$, $\mathbf{M}_{\mathbf{rs}}$, $\mathbf{M}_{\mathbf{qr}}$, $\mathbf{M}_{\mathbf{qq}}$, $\mathbf{M}_{\mathbf{qs}}$, $\mathbf{M}_{\mathbf{sr}}$, $\mathbf{M}_{\mathbf{sq}}$, $\mathbf{M}_{\mathbf{ss}}$ and the total added-mass matrix $\mathbf{M}_{\mathbf{AT}}$.

2.2 The calculation method of elements of added-mass matrix

The elements of added mass matrixes satisfy the Laplace equation and corresponding boundary condition. The Laplace equation can be solved using the analytical method for the simple geometric shape like an ellipsoid of revolution. While the geometric shape is arbitrary, the Laplace equation must be solved with numerical method.

In this paper, we use the panel method[11] (Fig. 1) to obtain the results of Laplace equation under the conditions of different boundary conditions. The panel method can quickly get the velocity potential distribution on the surface of the body through dividing the surface into some small panel meshes and distributing the singularity on every panel element. Through this approach, the Laplace equation can be change into the linear equations, the singularity strength and the velocity potential can be gotten through the velocity boundary condition on the surface of the body.

During the course of calculating the added-mass matrix, the $\mathbf{M}_{\mathbf{ri,r}}$, $\mathbf{M}_{\mathbf{ri,q}}$ and $\mathbf{M}_{\mathbf{ri,s}}$ can be obtained together, because they need the same velocity potential ψ_{ri}. $\mathbf{M}_{\mathbf{qs}}$ and $\mathbf{M}_{\mathbf{qq}}$ can be obtained together, because the same ψ_{qi} is needed. $\mathbf{M}_{\mathbf{ss}}$ can be got through the calculation of ψ_{si} and $\frac{\partial \psi_{si}}{\partial n}$.

3.0 THE VALIDATION OF THE CALCULATION METHOD

3.1 The added mass of an ellipsoid of revolution

For verifying the capability of the calculation method, we calculated the added masses of an ellipsoid of revolution with different fineness and the added-mass matrix of an approximate ellipsoid of

https://doi.org/10.1017/S0001924000008162 Published online by Cambridge University Press

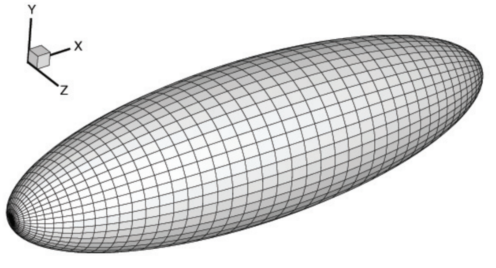

Figure. 1 The panel meshes.

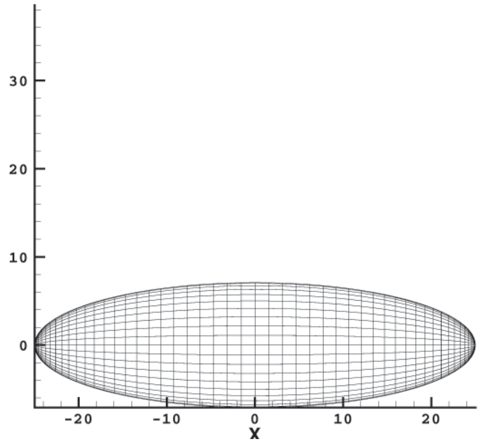

Figure 2. The approximate ellipsoid of revolution of Skyship-500.
(Long half-axes is 25·0m, Short half-axes is 7·09m, Length of airship is 50m).

Skyship-500 flexible airship. Through the comparison of calculated and theory results (Table 1), the calculation method can obtain the added mass very accurately.

The calculated conditions for ellipsoid of revolution:

- Model length: 2 metre; Density of air: 1·225kg/m^3;
- The airship surface along the x direction is divided into N1 = 50 parts.
- The circumference is divided into M1 = 40 parts.

3.2 The added mass of an approximate ellipsoid of Skyship-500

In Ref. 9, Yuwen Li has obtained the added mass matrix of Skyship-500 flexible airship using the ellipsoid analysis method. For verifying the capability of the proposed method in solving the added masses of the flexible body, we calculated the added masses of an approximate ellipsoid of Skyship-500 and compared with the analysis results (Fig. 2).

The calculation conditions: Model length: 50·0 m; Density of air: 1·158kg/m^3. The two normal mode shapes of the Skyship-500 airship were shown in Fig. 3.

The results of added mass matrix of the approximate ellipsoid of revolution of Skyship-500 airship using the analytical method in Ref. 9 are,

$$\mathbf{M}_{\mathbf{rs1}} = \begin{bmatrix} 0 & 0 & 0 & 0 \\ -1\cdot 2 & -4\cdot 3 & 0 & 0 \\ 0 & 0 & -1\cdot 2 & -4\cdot 3 \end{bmatrix}; \quad \mathbf{M}_{\mathbf{rs2}} = \begin{bmatrix} 0 & 0 & 0 & 0 \\ 0 & 0 & 92\cdot 7 & -30\cdot 9 \\ -92\cdot 7 & 30.9 & 0 & 0 \end{bmatrix}$$

$$M_{qq} = \begin{bmatrix} 0\cdot 75 & -0\cdot 14 & 0 & 0 \\ -0\cdot 14 & 0\cdot 96 & 0 & 0 \\ 0 & 0 & 0\cdot 75 & -0\cdot 14 \\ 0 & 0 & -0\cdot 14 & 0\cdot 96 \end{bmatrix}$$

The results of added mass matrix of the approximate ellipsoid of revolution Skyship-500 by the calculated method in this paper are,

https://doi.org/10.1017/S0001924000008162 Published online by Cambridge University Press

Table 1
The results of calculated and theory for different fineness ellipsoid of revolution

Fineness		m_{rr11}	m_{rr22}	m_{rr33}	m_{rr55}	m_{rr66}
	Calculation	2·608958	2·640051	2·64005	//	
1.0	Theory	2·565634	2·565634	2·565634	0·0	0·0
	Error (%)	1·688627	2·900531	2·900492	//	
	Calculation	0·2737721	0·9315569	0·9315571	7·926865E-02	7·926864E-02
2.0	Theory	0·2694	0·9034	0·9034	0·0768	0·0768
	Error (%)	1·622903	3·11677	3·116792	3·214387	3·214378
	Calculation	7·06128E-02	0·4728061	0·4728061	6·081234E-02	6·081232E-02
3.0	Theory	0·0695	0·4583	0·4583	0·0590	0·0590
	Error (%)	1·601151	3·165197	3·165197	3·071761	3·071724
	Calculation	2·654407E-02	0·2843911	0·2843910	4·267957E-02	4·267956E-02
4.0	Theory	0·0262	0·2757	0·2757	0·0414	0·0414
	Error (%)	1·313244	3·152376	3·152339	3·090742	3·090722
	Calculation	1·230887E-02	0·1892188	0·1892187	3·076247E-02	3·076248E-02
5.0	Theory	0·0121	0·1835	0·1835	0·0299	0·0299
	Error (%)	1·726182	3·116512	3·116458	2·884525	2·884555
	Calculation	6·529992E-03	0·1347236	0·1347236	2·298685E-02	2·298686E-02
6.0	Theory	0·0064	0·1307	0·1307	0·0223	0·0223
	Error (%)	2·031131	3·0785	3·0785	3·080067	3·080103
	Calculation	1·076165E-03	5·062717E-02	5·06272E-02	9·400066E-03	9·400068E-03
10.0	Theory	0·0011	0·0493	0·0493	0·0092	0·0092
	Error (%)	-2·16683	2·692024	2·692047	2·17463	2·174651

$$M_{rs} = \begin{bmatrix} M_{rs1(3\times N)} \\ M_{rs2(3\times N)} \end{bmatrix} = \begin{bmatrix} 2\cdot 8622036\text{E-}08 & -1\cdot 1903893\text{E-}06 & 5\cdot 6440674\text{E-}09 & 4\cdot 4376120\text{E-}06 \\ \mathbf{1\cdot 124520} & \mathbf{4\cdot 343076} & -1\cdot 0938199\text{E-}07 & -8\cdot 6906368\text{E-}07 \\ -8\cdot 4545391\text{E-}08 & -3\cdot 2512567\text{E-}06 & \mathbf{1\cdot 164359} & \mathbf{4\cdot 325747} \\ 0\cdot 0 & 0\cdot 0 & 0\cdot 0 & 0\cdot 0 \\ 1\cdot 9527299\text{E-}06 & 8\cdot 2762841\text{E-}07 & \mathbf{94\cdot 86114} & \mathbf{-32\cdot 44128} \\ \mathbf{-94\cdot 86111} & \mathbf{32\cdot 44129} & -5\cdot 9547001\text{E-}06 & 8\cdot 5480121\text{E-}07 \end{bmatrix}$$

$$\mathbf{M}_{\mathbf{qq}} = \begin{bmatrix} \mathbf{0\cdot 7387686} & \mathbf{-0\cdot 1389143} & -1\cdot 2898592\text{E-}08 & 1\cdot 8662071\text{E-}08 \\ \mathbf{-0\cdot 1389381} & \mathbf{0\cdot 9323495} & -9\cdot 5466204\text{E-}09 & 1\cdot 0757031\text{E-}08 \\ -4\cdot 4279300\text{E-}09 & -1\cdot 9317689\text{E-}08 & \mathbf{0\cdot 7387685} & \mathbf{-0\cdot 1389142} \\ -2\cdot 5144043\text{E-}08 & -3\cdot 5526564\text{E-}09 & \mathbf{-0\cdot 1389381} & \mathbf{0\cdot 9323496} \end{bmatrix}$$

From the comparison of results of added-mass matrix calculated by the panel method and theory method, we can see that the panel method can calculate the added-mass matrix for flexible airship very accurately.

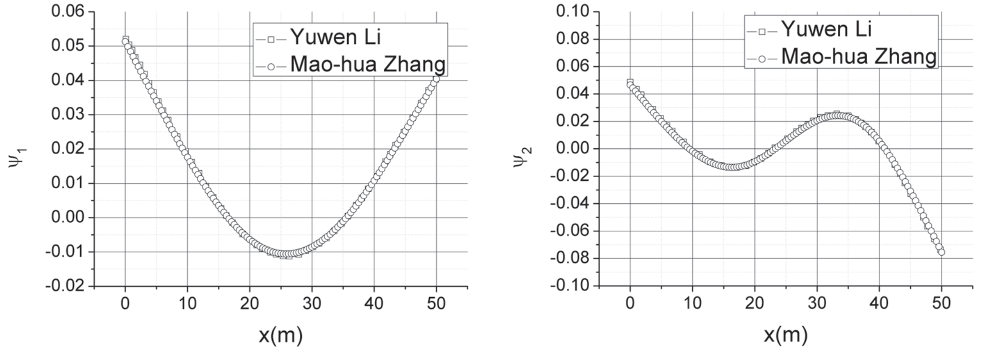

(a) First mode shape (b) Second mode shape

Figure 3. The two normal mode shapes of Skyship-500 airship.

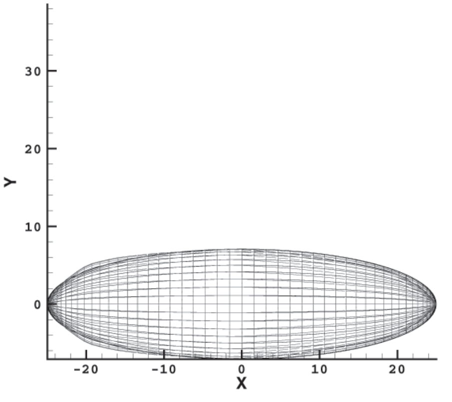

Figure 4. The Skyship-500 (green) and its approximate ellipsoid of revolution (red).

4.0 THE DIFFERENCE OF ADDED-MASS WITH GEOMETRIC SHAPE

In this section, for analysis the difference of added-mass with geometric shape and explaining the ability of the proposed method, we calculated all added-mass matrixes of the real Skyship-500 airship and its own approximate ellipsoid of revolution (Fig. 4) with two same normal mode shapes by the proposed method.

The difference in geometry shape of Skyship-500 airship and approximate ellipsoid of revolution shown in Fig. 4 is located at the head and tail of the airship hull. The radius of generatrix of head of Skyship-500 airship is bigger than the approximate ellipsoid of revolution, while the radius of generatrix of airship tail is less than the approximate ellipsoid of revolution. Using the theory method based on the ellipsoid of revolution, the influence of change of geometry with same fineness on the added-mass matrix cannot be obtained. Because of using the real geometry shape, this influence of change of geometry with same fineness can be obtained by panel method. We used the Skyship-500 shape and its approximate ellipsoid of revolution to analysis the difference of added-mass matrix with the change of geometry shape with same fineness.

https://doi.org/10.1017/S0001924000008162 Published online by Cambridge University Press

Table 2
Results of added mass matrix for Skyship-500 airship and its approximate ellipsoid of revolution

Element of mass matrix	Skyship-500 airship	Ellipsoid of revolution	Difference (%)	Element of added mass matrix	Skyship-500 airship	Ellipsoid of revolution	Difference (%)
M_{rr11}	601·0674	603·0719	0·33349	M_{qq11}, M_{qq33}	0·71243	0·7387	3·68738
M_{rr22}	5,061·977	5262·213	3·955688	M_{qq12}, M_{qq34}	-7·867e-2	-0·1389	76·56032
M_{rr33}	5,061·976	5262·213	3·955708	M_{qq21}, M_{qq43}	-7·847e-2	-0·1389	77·01032
M_{rr55}	446,583·1	465359·5	4·204458	M_{qq22}, M_{qq44}	0·81064	0·9323	15·00789
M_{rr66}	446,583·3	465359·5	4·204412	M_{qs11}, M_{qs33}	3·777e-2	2·6175e-2	-30·699
M_{rq21}, M_{rq33}	15·51168	15·52761	0·102697	M_{qs12}, M_{qs34}	0·16056	0·17313	7·828849
M_{rq22}, M_{rq34}	7·06528	17·77954	4·185457	M_{qs21}, M_{qs43}	-2·173e-2	-1·905e-2	-12·3332
M_{rq53}, $-M_{rq61}$	170·2216	113·699	-33·2053	M_{qs22}, M_{qs44}	-2·295e-2	-3·881e-2	69·10675
M_{rq54}, M_{rq62}	-55·0505	-33·01368	-40·0302	M_{ss11}, M_{qs33}	1·9614e-2	1·9927e-2	1·595799
M_{rq21}, M_{rq33}	2·076484	1·12452	-45·845	M_{ss12}, M_{qs34}	-2·031e-3	-5·527e-3	172·132
M_{rq22}, M_{rq34}	3·771714	4·343076	15·1486	M_{ss21}, M_{qs43}	-2·027e-3	-5·527e-3	172·669
M_{rq53}, M_{rq61}	92·47656	94·86114	2·578578	M_{ss22}, M_{qs44}	4·513e-2	5·5052e-2	21·98538
M_{rq54}, M_{rq62}	-14·5703	-32·44128	122·6535				

Through calculation of the added-mass matrix of Skyship-500 shape and its own approximate ellipsoid of revolution, the results of some elements of the added-mass matrix were shown in the following table, other elements of the added-mass matrix are very small and they can be seen as zero in the dynamic model of flexible airship.

From the results shown in Table 2, we can see that the difference in the shape of the airship hull will change some elements of added-mass matrix. For the elements of the added-mass matrix of rigid body, the geometric shape mainly affects the $\mathbf{M_{rr22}}$, $\mathbf{M_{rr33}}$, $\mathbf{M_{rr55}}$, $\mathbf{M_{rr66}}$. The other elements of the added-mass matrix of flexible body such as $\mathbf{M_{rq}}$, $\mathbf{M_{rs}}$, $\mathbf{M_{qq}}$ and $\mathbf{M_{qs}}$ are very sensitive to the hull shape. Although the hull shape has some effect on the elements of $\mathbf{M_{ss}}$, the differences have little effect on the dynamic characteristics of airship due to the very small value of .

From the comparison of the results of real Skyship-500 airship shape and its own approximate ellipsoid of revolution, we can see that the panel method can obtain the effect of the change of geometry shape on the added-mass matrixes.

The velocity potential distribution with different boundary condition as illustrated in Figs 5-7. From the velocity potential distribution shown in Figs 5-7, we can see that the velocity potentials associated with the rigid-body motion $\mathbf{\Psi_r}$, related to the mode shapes $\mathbf{\Psi_q}$ and associated with the slopes of the mode shape functions $\mathbf{\Psi_s}$ satisfy $\mathbf{\Psi_r} > \mathbf{\Psi_q} > \mathbf{\Psi_s}$. This makes the value of corresponding elements of added-mass matrix have the law:

$$M_{rr} > M_{rq} > M_{rs} > M_{qq} > M_{qs} > M_{ss}$$

For velocity potential ψ_{r2}, ψ_{r6}, ψ_{q1}, ψ_{q2}, ψ_{s1} and ψ_{s2}, the distribution is symmetric distribution about the x-z plane but the sign will be changed, respectively. Similarly, for velocity potential

https://doi.org/10.1017/S0001924000008162 Published online by Cambridge University Press

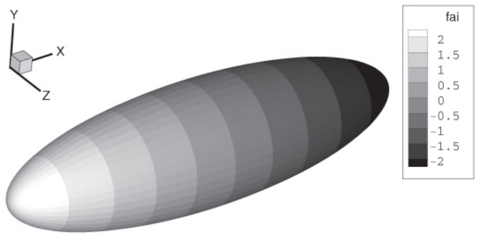

(a) ψ_{r1} with $\frac{\partial \psi_{r1}}{\partial n} = n_1$

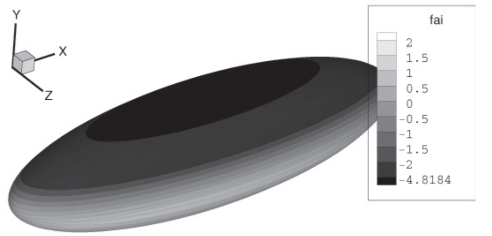

(b) ψ_{r2} with $\frac{\partial \psi_{r2}}{\partial n} = n_2$

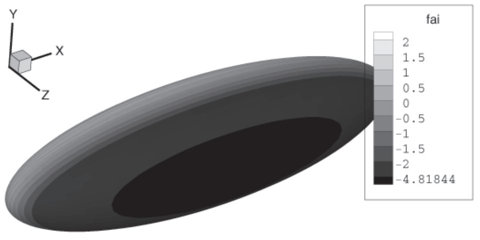

(c) ψ_{r3} with $\frac{\partial \psi_{r3}}{\partial n} = n_3$

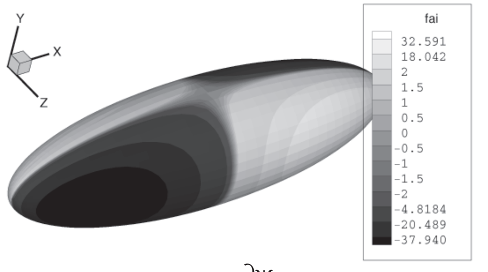

(d) ψ_{r4} with $\frac{\partial \psi_{r5}}{\partial n} = zn_1 - xn_3$

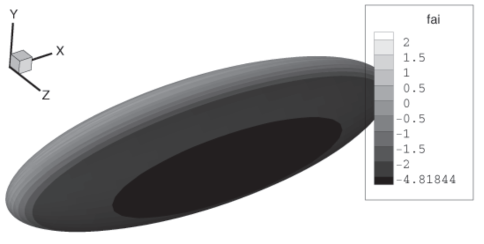

(e) ψ_{r5} with $\frac{\partial \psi_{r6}}{\partial n} = -yn_1 + xn_2$

Figure 5. The velocity potential ψ_r distribution of ellipsoid of revolution.

ψ_{r3}, ψ_{r5}, ψ_{q3}, ψ_{q4}, ψ_{q5} and ψ_{s4}, the distribution is symmetric distribution about the *x-y* plane, the sign will be changed, too.

From the velocity potential $\mathbf{\Psi_q}$ distribution shown in Fig. 6, we can see that the distribution is decided by the mode shape. The curve of the first mode shape along the *x* axis (Fig. 3) is approximate parabola, so the velocity potential distribution of ψ_{q1} and ψ_{q3} is less at two ends of the ellipsoid of revolution and bigger on the middle part. The trend of the second mode shape along the x axis (Fig. 3) decided the trend of the velocity potential ψ_{q2} and ψ_{q4} similarly.

The velocity potential $\mathbf{\Psi_s}$ reflects the change of the slopes of the mode shape functions. From the velocity potential distribution of ψ_{s1} and ψ_{s3} shown in Fig. 7, we can see that the distribution trends are consistent with the change of slope of first mode shape along the *x* axis. The distribution trends of ψ_{s2} and ψ_{s4} shown in Fig. 7 are consistent with the change of slope of second mode shape along the *x* axis, too.

https://doi.org/10.1017/S0001924000008162 Published online by Cambridge University Press

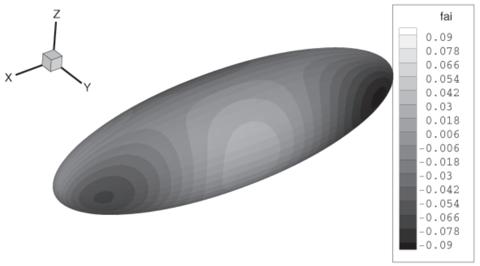

(a) (ψ_{q1} with $\frac{\partial \psi_{q1}}{\partial n} = \Phi_1^T n$)

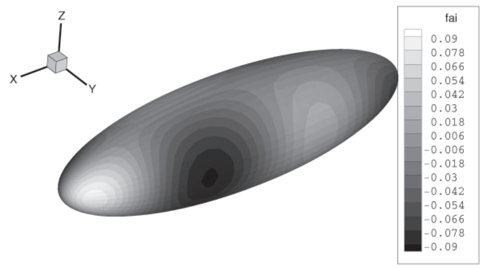

(b) (ψ_{q2} with $\frac{\partial \psi_{q2}}{\partial n} = \Phi_2^T n$)

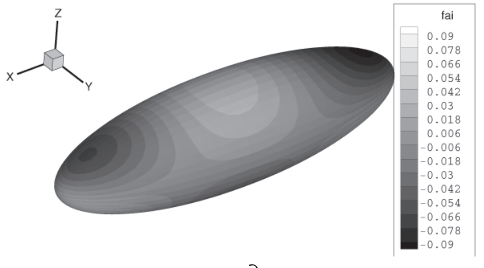

(c) (ψ_{q3} with $\frac{\partial \psi_{q3}}{\partial n} = \Phi_3^T n$)

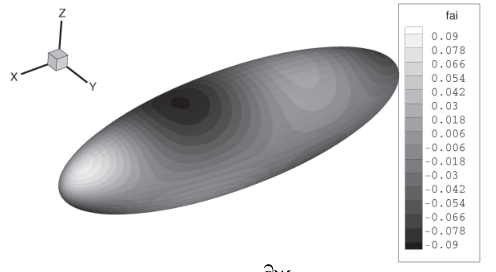

(d) (ψ_{q4} with $\frac{\partial \psi_{q4}}{\partial n} = \Phi_4^T n$)

Figure 6. The velocity potential ψ_q distribution of ellipsoid of revolution.

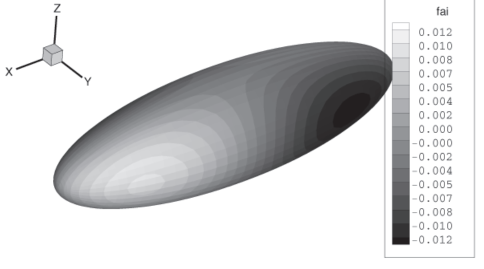

(a) (ψ_{s1} with $\frac{\partial \psi_{s1}}{\partial n} = \Phi_1'^T n$)

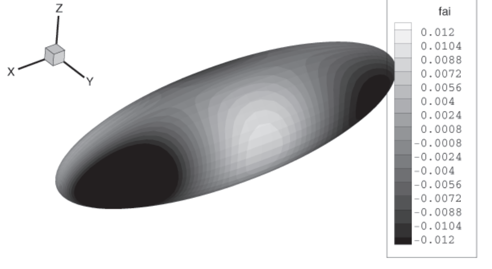

(b) (ψ_{s2} with $\frac{\partial \psi_{s2}}{\partial n} = \Phi_2'^T n$)

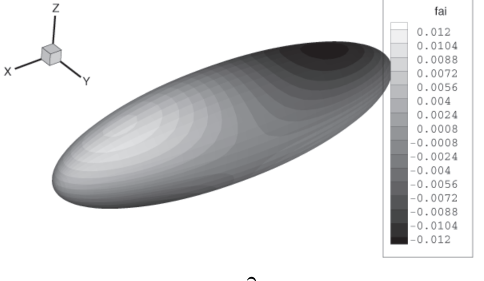

(c) (ψ_{s3} with $\frac{\partial \psi_{s3}}{\partial n} = \Phi_3'^T n$)

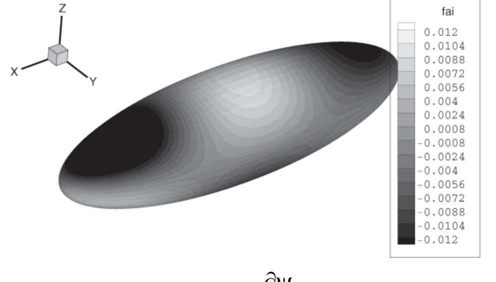

(d) (ψ_{s4} with $\frac{\partial \psi_{s4}}{\partial n} = \Phi_4'^T n$)

Figure 7. The velocity potential ψ_s distribution of ellipsoid of revolution.

https://doi.org/10.1017/S0001924000008162 Published online by Cambridge University Press

5.0 CONCLUSIONS

The flexibility of stratosphere airship is very important due to the huge volume, length and relatively small pressure difference thinking of the structure material characteristics and helium leakage. During the course of building the flight dynamic model for such vehicle, the deformation must be considered. The added-masses of flexible airship are one part of the dynamic model.

For obtaining the added masses of the arbitrary flexible airship, in this paper, we proposed an approach that can obtain the added mass for flexible airship. The panel method was used to solve the Laplace equation with different boundary conditions. Through the comparison of results of computation and theory for ellipsoid of revolution and the flexible Skyship-500 airship, the proposed method can calculate the added-mass matrix accurately for arbitrary geometry shape and consider the variety of geometric shapes.

ACKNOWLEDGMENT

The presented work was supported by National Natural Science Fundation of China (No.61175074).

REFERENCES

1. GOMES, S.B.V. and RAMOS, J.G. Airship dynamic modeling for autonomous operation, 1998, Proceedings of the 1998 IEEE International Conference on Robotics & Automation, pp 3462-3467.
2. ASHRAF, Z. and CHOUDHRY, M.A. Dynamic modeling of the airship using analytical aerodynamic model, 2009, 2009 International Conference on Emerging Technologies, pp 188-193.
3. CAI, Z-L.Q. and XI, W.Y. Dynamic modeling for airship equipped with ballonets and ballast, *Applied Math and Mech*, 2005, **26**, (8), pp 1072-1082.
4. PEDDIRAJU, P. LIESK, T. and NAHON, M. Dynamics modeling for an unmanned, unstable, fin-less airship, 2009, 18th AIAA light-than-air systems technology conference, AIAA 2009-2862, pp 1-18.
5. AZINHEIRA, J. R., DE PAIVA, E.C and BUENO, S.S. Influence of wind speed on airship dynamics, *J Guidance, Control and Dynamics*, 2002, **25**, (6), pp 1116-1124.
6. LI, Y. and NAHON, M. Modeling and simulation of airship dynamics, *J Guidance, Control and Dynamics*, 2007, **30**, (6), pp 1691-1700.
7. SCHMIDT, D.K. Modeling and near-space station keeping control of a large high-altitude airship, *J Guidance, Control and Dynamics*, 2007, **30**, (2), pp 540-547.
8. LI, Y., NAHON, M. and SHARF, I. Dynamics modeling and simulation of flexible airships, *AIAA J*, 2009, **47**, (3), pp 592-605.
9. LI, Y. Dynamics Modeling and Simulation of Flexible Airships, 2008, PhD thesis.
10. LAMB, H. *Hydrodynamics*, Dover, New York, Sixth edition, 1945, pp 160-201.
11. HESS, J.L. and SMITH, A.M.O. Calculation of potential flow about arbitrary bodies, *Prog in Aeronautical Science*, 1967, pp 1-138.

https://doi.org/10.1017/S0001924000008162 Published online by Cambridge University Press